crystals

MDPI

Article

Dislocation Creep: Climb and Glide in the Lattice Continuum

Sinisa Dj. Mesarovic

School of Mechanical and Materials Engineering, Washington State University, Pullman, WA 99164, USA; mesarovic@mme.wsu.edu

Received: 9 June 2017; Accepted: 31 July 2017; Published: 4 August 2017

Abstract: A continuum theory for high temperature creep of polycrystalline solids is developed. It includes the relevant deformation mechanisms for diffusional and dislocation creep: elasticity with eigenstrains resulting from vacancy diffusion, dislocation climb and glide, and the lattice growth/loss at the boundaries enabled by diffusion. All the deformation mechanisms are described with respect to the crystalline lattice, so that the continuum formulation with lattice motion as the basis is necessary. However, dislocation climb serves as the source sink of lattice sites, so that the resulting continuum has a sink/source of its fundamental component, which is reflected in the continuity equation. Climb as a sink/source also affects the diffusion part of the problem, but the most interesting discovery is the climb-glide interaction. The loss/creation of lattice planes through climb affects the geometric definition of crystallographic slip and necessitates the definition of two slip fields: the true slip and the effective slip. The former is the variable on which the dissipative power is expanded during dislocation glide and is thus, the one that must enter the glide constitutive equations. The latter describes the geometry of the slip affected by climb, and is necessary for kinematic analysis.

Keywords: dislocation climb; lattice sink; vacancy sink; continuum with a material sink; climb-glide interaction

1. Introduction

At high temperatures, polycrystalline solids exhibit creep—a slow, phenomenologically viscous flow. The basic deformation mechanisms are either directly or indirectly associated with vacancy diffusion [1,2]. In purely diffusional creep, the prominent feature is the lattice growth/loss at the boundaries [3–5]. A common view of dislocation creep is that deformation is accomplished by climb-assisted glide [6], whereby climb only assists in bypassing the obstacles and contributes little to the overall deformation. The climb-only deformation mechanism has been proposed early [7], but the experimental evidence has been accumulating slowly. The climb appears to be a standalone deformation mechanism producing (under some conditions) significant creep strains in: *hcp* metals [8], intermetallics and superalloys [9], quasicrystals [10], and the Earth's lower mantle rocks under high pressure and high temperature conditions [11]. Moreover, the interactions of dislocations and vacancies are of particular importance in irradiated metals [12]. In view of the uncertainties in the proposed mechanisms for high temperature creep, it seems reasonable to aim at a mathematical model that can describe the concurrent operation of glide, climb, and diffusion, with each mechanism contributing significant strains. This is the purpose of the present communication.

1.1. Mass Continuum

The standard mathematical definition of the continuum begins with the statement: At instant t, *material* point (element) currently at the position $\mathbf{x}$ is moving with the velocity $\overline{\mathbf{v}}(\mathbf{x}, t)$. This brings up the question—what is the physical meaning of the *material*? In fluid mechanics treatises, the answer is

typically mathematical rather than physical; material is identified with mass. Such continuum will be called *mass continuum* (Quantities and operators specific to the mass continuum are marked with an overbar to distinguish them from their analogues in the lattice continuum.).

Specifically, the mass density field $\rho(\mathbf{x}, t)$ is convected with the velocity $\overline{\mathbf{v}}(\mathbf{x}, t)$. Owing to the continuous mixing of fluid atoms, the material (point) is not associated with a specific (group of) atom(s). In single- or multi-component fluids, the barycentric velocity preserves the linear momentum of the assembly of atoms (e.g., [13]), thus yielding (with application of the transport theorem) the simple and elegant continuum version of Newton's 2nd law—the Cauchy equations of motion:

$$\nabla \cdot \overline{\boldsymbol{\sigma}} + \rho \mathbf{g} = \rho \frac{\overline{D}\mathbf{v}}{Dt}. \tag{1}$$

The operator ∇ is the gradient operator, $\overline{\boldsymbol{\sigma}}$ is the Cauchy stress (in the mass continuum), $\mathbf{g}$ is the gravitational acceleration and $\overline{D}/Dt$ is the material derivative (in the mass continuum). The equations of motion (1) also indicate why the mass density (among all other continuum fields) plays a special role. Further, in the absence of nuclear reaction, the mass is conserved, so that the continuity equation is identified with the local mass conservation condition:

$$\frac{\overline{D}\rho}{Dt} = -\rho \nabla \cdot \overline{\mathbf{v}}. \tag{2}$$

Finally, we note that all of the above refers to the Eulerian (spatial) description of the continuum. The failure to identify the material with a physical entity renders any Lagrangean (material) description meaningless.

1.2. Lattice Continuum

In solid mechanics problems, where Lagrangean kinematics is essential, such formulation does not stand up to scrutiny, unless one assumes the complete absence of mixing/diffusion, in which case the material point is identified with a particular set of atoms. In crystalline solids, the relevant deformation mechanisms are referred to the crystalline lattice. For example, the plastic slip is produced by the motion of dislocations with respect to the lattice, while the elastic deformation is associated with lattice stretching. Thus, the fundamental developments in crystal elasto-plasticity [14–17] are, in fact, based on the *lattice continuum* without diffusion, which is equivalent to the mass continuum, so that the nature of the continuum is not emphasized.

In the solid mechanics problems with diffusion, the importance of crystalline lattice was noted early by Larché and Cahn [18–20] but in the form of lattice constraint imposed on the otherwise mass-based continuum. Berdichevsky et al. [21] noted the absence of Lagrangean description in the mass continuum, specifically for the newly grown lattice at the grain boundary.

When diffusion and diffusion-mediated processes control the deformation of solids, the overall deformation process is expected to be quasi-static. The rate of change of linear momentum in (1) is considered negligible, so that the governing mechanical equations are the equilibrium conditions. The need for equivalence of atomic and continuum linear momenta being thus eliminated, the lattice continuum formulation becomes natural. Elements of the lattice continuum were introduced by Garikipati et al. [22], but the full formulation of the lattice continuum for Nabarro–Herring creep was developed only recently [23]. It includes the lattice versions of the material derivative and the transport theorem, as well as the definition of Lagrangean coordinates for the newly created lattice. The limitation of this formulation is that lattice growth/loss is confined to the grain boundary; in the bulk of the crystal, the lattice version of the continuity equation is equivalent to the local conservation of lattice density. In this paper, we extend the formulation to the problem of dislocation climb, whereby climbing edge dislocations serve as the sink/source of the lattice throughout the bulk of the crystal. Thus, the resulting continuum embodies a sink/source of the material. This appears to be an entirely new concept (The analogous mass continuum would be the one where deformation is accompanied by

nuclear reaction (mass sink). One can envision such problems arising in case of load bearing nuclear fuel, but this author is not aware of any such developments.).

The problem considered here is the concurrent operation of dislocation glide, climb and vacancy diffusion, the latter two being intrinsically linked. The vacancy diffusion is also inseparable from the lattice growth at grain boundaries (barring awkward assumptions), so that the problem considered is the concurrent operation of dislocation creep and Nabarro–Herring creep. The paper is organized as follows.

In Section 2, the kinematics of lattice continuum with lattice sink/source, diffusion, dislocation glide and climb is developed. In addition to the lattice sink, the kinematic interaction between glide and climb is a novel element. Power balance (for an isothermal process) is formulated in Section 3. In Section 4, the weak form of the problem is formulated directly from the power balance using the principle of virtual power, followed by the strong form. While many components of the strong form turn out to be familiar from the literature, the glide-climb interaction is a novel concepts and is discussed in some detail. The conclusions are given in Section 5.

2. Kinematics

At high temperatures, vacancy diffusion takes place by the vacancy-atom exchange mechanism, thus producing the complementary fluxes of atoms and vacancies. Crystal boundaries serve as sources and sinks of vacancies resulting in lattice growth/loss on the boundary faces under tension/compression. The diffusion and lattice growth in the Nabarro–Herring creep is illustrated in Figure 1. The lattice continuum corresponding to the Nabarro–Herring creep has been formulated [23] and includes the Eulerian and Lagrangean descriptions of the newly formed lattice.

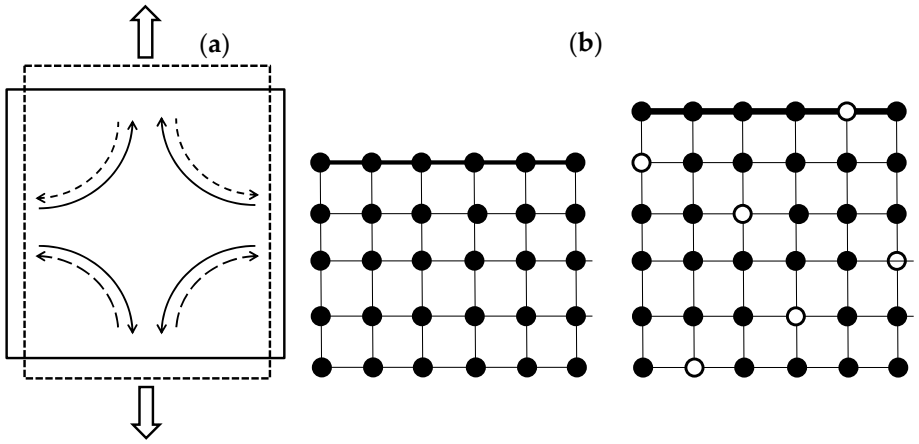

Figure 1. (**a**) Schematic representation of vacancy diffusion (dashed lines) and atom diffusion (solid lines) within a crystalline grain leading to the creation of new lattice planes at the boundary under tension and disappearance of lattice planes at other boundaries. (**b**) Schematic illustration of the creation of a new lattice plane. Thick solid line represents crystal boundary, solid and hollow circles are atoms and vacancies. Initial vacancy-free crystal (left) absorbs vacancies from the boundary (in exchange for atoms). The new configuration (right) has an extra lattice plane and extra vacancies which then diffuse through the bulk towards the disappearing boundaries. Diffusion of atoms and vacancies takes place by the vacancy-atom exchange mechanism.

We consider two species occupying lattice sites: atoms and vacancies; without interstitials. At any instant t, the lattice velocity field $\mathbf{v}(\mathbf{x}, t)$ is defined on an open domain Ω, its closure $\partial\Omega$ having the outer normal $\mathbf{n}$. The lattice velocity gradient $\mathbf{L}(\mathbf{x}, t)$ is defined as:

$$\mathbf{L} = \frac{\partial \mathbf{v}}{\partial \mathbf{x}} = \mathbf{v}\nabla; L_{ij} = \frac{\partial v_i}{\partial x_j} = v_{i,j}\,. \tag{3}$$

2.1. Dislocation Climb and the Continuity Equation

The mechanism of dislocation climb consists of vacancy absorption by the dislocation core. As the vacancy is absorbed, the core of edge dislocation moves one atomic space and one lattice position is lost. Thus, the dislocation climb mechanism, illustrated in Figure 2a, represents the lattice sink, as well as the vacancy sink. Therefore, the continuity equation, i.e., the lattice balance law, must now include—not only the convection of lattice sites, but also the local sink strength. Let the lattice site density be $N_L(\mathbf{x}, t)$ and let $\dot{s}(\mathbf{x}, t)$ be the fraction of lattice sites lost per unit time. Then:

$$\frac{\partial N_L}{\partial t} = -\nabla \cdot (\mathbf{v} N_L) - N_L \dot{s}. \tag{4}$$

with reference to Figure 2a, it is clear that there is no kinematic constraint restricting the climb motion to one direction: dislocation can climb or descend, operating as sink or source of lattice sites and vacancies. The convention adopted here with positive $\dot{s}$ representing climb/sink conforms to the usual representation of climb in the literature.

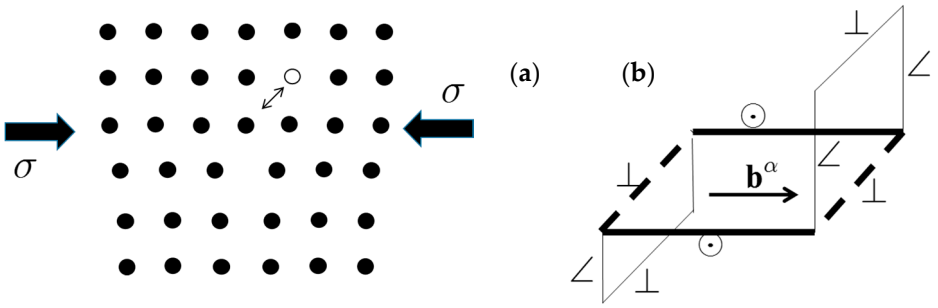

Figure 2. (**a**) Edge dislocation and vacancy (hollow circle). The vacancy-atom exchange takes place. Dislocation climbs and a lattice point disappears. (**b**) Illustration of climb starting from a planar dislocation loop with the Burgers vector $\mathbf{b}^\alpha$ (thick lines). The screw components ($\odot$) don't climb. The climb of initial edges ($\perp$) produces parallel edges as well as out-of-plane edge segments ($\angle$) which cannot glide. As both parallel and out-of-plane edges continue to climb, the loop expands and operates as climb analogue of the Frank–Read source.

The material (lattice) derivative of any material field $Y(\mathbf{x}, t)$ is

$$\frac{DY}{Dt} = \frac{\partial Y}{\partial t} + \mathbf{v} \cdot \nabla Y, \tag{5}$$

so that:

$$\frac{DN_L}{Dt} = \frac{\partial N_L}{\partial t} + \mathbf{v} \cdot \nabla N_L = -N_L \nabla \cdot \mathbf{v} - N_L \dot{s}. \tag{6}$$

The glide of dislocations has been studied in detail, including the interactions between dislocations on different slip systems, as well as dislocation multiplication and strain hardening mechanisms [24–26]. Here we focus on dislocation climb and its interactions with dislocation glide.

The slip system α is described by a triad of unit orthogonal vectors: the slip direction $\mathbf{s}^\alpha = \mathbf{b}^\alpha / |\mathbf{b}^\alpha|$, the slip plane normal $\mathbf{m}^\alpha$, and $\mathbf{t}^\alpha = \mathbf{s}^\alpha \times \mathbf{m}^\alpha$. The evolution of climbing edge dislocations, starting from a rectangular dislocation loop on the slip system α is illustrated in Figure 2b. Evidently, the climb of original edges produces, not only the parallel edge segments ($\perp$), but also the out-of-plane edge segments ($\angle$) which cannot glide. Further climb by all edges results in a multiplication mechanism analogous to the Frank–Read source for glide. Let θ^α be the density (length per volume) of all edge dislocations ($\perp$ and $\angle$) associated with the slip system α, and let v^α_{climb} be the average climb velocity

for edges belonging to the slip system. Then, in analogy with the Orowan equation for the slip rate, the strength of the lattice sink associated with the slip system α is

$$\dot{s}^{\alpha} = \theta^{\alpha} v^{\alpha}_{\text{climb}} b^{\alpha}; b^{\alpha} = |\mathbf{b}^{\alpha}|, \tag{7}$$

and the total lattice sink strength is obtained by summation over all slip systems:

$$\dot{s} = \sum_{\alpha} \dot{s}^{\alpha}. \tag{8}$$

2.2. Elastic–Plastic Decomposition

In addition the lattice density $N_L(\mathbf{x}, t)$, the material (lattice) point currently located at $\mathbf{x}$, carries the vacancy concentration $c(\mathbf{x}, t)$, i.e., the fraction of lattice sites occupied by vacancies, and the deformation gradient $\mathbf{F}(\mathbf{x}, t)$:

$$\frac{D}{Dt}\mathbf{F} = \mathbf{L} \cdot \mathbf{F}. \tag{9}$$

To extend the definition of lattice-advected variables to the lattice being currently created, it is sufficient to assert the continuity of deformation gradient, vacancy concentration and lattice density, within the crystal [23]. The key elements of the Lagrangean (spatial) description are thus defined. The reference configuration $\mathbf{X}$ can, in principle, be obtained from the current configuration, but it will be fictitious for the lattice grown during the process. The mapping $\mathbf{x} \to \mathbf{X}$ is multiple-valued, with gaps and overlaps at grain boundaries and inside the grain.

The deformation gradient tensor can be decomposed into the elastic-compositional deformation gradient $\mathbf{F}^*$, and the plastic deformation gradient $\mathbf{F}^p$. The former represents the motion which produces a deformed lattice topologically equivalent to the reference lattice, the latter changes the topology, i.e., it accounts for both–glide and climb of dislocations. The decomposition is multiplicative and formally identical to the standard (glide-only) elastic–plastic decomposition [14]:

$$\mathbf{F} = \mathbf{F}^* \cdot \mathbf{F}^p. \tag{10}$$

However, the plastic gradient now includes the climb deformation, so that

$$F^p = \det \mathbf{F}^p \neq 1. \tag{11}$$

Following the decomposition (10), the velocity gradient (3) is decomposed in elastic-compositional and plastic portions:

$$\mathbf{L} = \mathbf{L}^* + \mathbf{L}^p = \dot{\mathbf{F}}^* \cdot \mathbf{F}^{*-1} + \mathbf{F}^* \cdot \underbrace{\dot{\mathbf{F}}^p \cdot \mathbf{F}^{p-1}}_{\widetilde{\mathbf{L}}^p} \cdot \mathbf{F}^{*-1}. \tag{12}$$

The decompositions (10) and (12) reflect the imaginary sequential deformation. First, the reference lattice is deformed to intermediate (isoclinic) configuration without changing the symmetry of the lattice, $\mathbf{F}^p : \mathbf{X} \to \widetilde{\mathbf{x}}$. In contrast to standard crystal plasticity based on dislocation glide, here the lattice planes are lost/created, resulting in the translational motion of the parts of the lattice, but preserving the lattice symmetries and orientation (hence the attribute isoclinic still applies). Then, the intermediate configuration is transformed into the current configuration, $\mathbf{F}^* : \widetilde{\mathbf{x}} \to \mathbf{x}$. In the glide-only elasto-plasticity, while the two steps are not represented by 1–1 mappings (i.e., the tensors $\mathbf{F}^p$ and $\mathbf{F}^*$ are not compatible), the total deformation gradient $\mathbf{F}$ represents 1–1 mapping $\mathbf{x} \leftrightarrow \mathbf{X}$. This is clearly not the case here: the mapping $\mathbf{F}^{-1} : \mathbf{x} \to \mathbf{X}$ is multiple-valued and discontinuous. (Note that in the glide-only plasticity, the incompatibility of $\mathbf{F}^*$ can be considered as the consequence of incompatibility of $\mathbf{F}^p$, arising from the requirement that the total deformation gradient be compatible. In the absence of dislocation glide ($\mathbf{F}^p = \mathbf{I}$), $\mathbf{F}^*$ is compatible.)

Let the lattice density and elementary volume in intermediate configuration be $\widetilde{N}_L$ and $d\widetilde{\Omega}$. Then, elastic-compositional changes between intermediate and current configurations can be expressed as

$$F^* N_L = \widetilde{N}_L; d\Omega = F^* d\widetilde{\Omega}; F^* = \det \mathbf{F}^*. \tag{13}$$

Note that we first define all fields (including deformation gradient) in the current configuration, e.g., $Y(\mathbf{x})$, which is the only configuration where the position vector $\mathbf{x}$ represents one and only one material (lattice) point. To minimize the notational clutter, we write $Y(\mathbf{x}) = Y(\widetilde{\mathbf{x}})$ $(\mathbf{F}^* : \widetilde{\mathbf{x}} \to \mathbf{x})$ and freely switch the domains of integration between the current and intermediate configurations:

$$\int_{\Omega} Y(\mathbf{x}) d\Omega = \int_{\widetilde{\Omega}} F^* Y(\widetilde{\mathbf{x}}) d\widetilde{\Omega}. \tag{14}$$

(Although the equality (14) is widely used in the literature on elasto-plasticity, in view of the multiple-valuedness of the mapping $\mathbf{F}^{*-1} : \mathbf{x} \to \widetilde{\mathbf{x}}$, the meaning of the integral on the right is not obvious. The clarifying point is that $\mathbf{F}^*$ includes only lattice stretching and rotation so that the mapping of lattice points is 1–1; only the mapping of coordinates is multiple-valued. The function $Y(\widetilde{\mathbf{x}})$ is understood to be defined on lattice points (as opposed to coordinates), with the corresponding interpretation of the integral. In contrast to glide-only plasticity, the analogous transformation to the reference configuration is meaningless here.)

The plastic velocity gradient on intermediate configuration $\widetilde{\mathbf{L}}^p$ in (12) accounts for changes in lattice topology and is defined from the elementary slip system state variables: slip rate $\dot{\gamma}^\alpha$ and climb rate (lattice sink strength) $\dot{s}^\alpha$:

$$\widetilde{\mathbf{L}}^p = \sum_\alpha \dot{\gamma}^\alpha \widetilde{\mathbf{s}}^\alpha \widetilde{\mathbf{m}}^\alpha - \sum_\alpha \dot{s}^\alpha \widetilde{\mathbf{s}}^\alpha \widetilde{\mathbf{s}}^\alpha, \tag{15}$$

where the vectors $\widetilde{\mathbf{s}}^\alpha$ and $\widetilde{\mathbf{m}}^\alpha$ are unit and orthogonal in the intermediate configuration. The choice between intermediate and current configurations as the basis for definition of slip has been extensively discussed in literature [15–17].

2.3. Climb–Glide Interaction

When dislocation climb is present, the scalar fields $\gamma^\alpha(\mathbf{x}, t)$ have a different physical (geometric) meaning then in the glide-only case, which has implications on the constitutive relations. Define the true slip field $\hat{\gamma}^\alpha(\mathbf{x}, t)$ as the slip occurring without any climb. This is the variable that corresponds to the standard crystal plasticity slip field. As illustrated in Figure 3, the loss of lattice planes parallel to the slip plane affects the effective slip $\gamma^\alpha(\mathbf{x}, t)$ directly. (An analogous continuum illustration of the same phenomenon is shown in Figure 4 in Section 4.) The loss of lattice planes orthogonal to the slip plane only affects the gradient of slip $\nabla\gamma^\alpha$, which is accounted for implicitly through the loss of lattice (6).

The relation between true slip rate $\dot{\hat{\gamma}}^\alpha$ and effective slip rate $\dot{\gamma}^\alpha$ is derived in Appendix A:

$$\frac{\dot{\gamma}^\alpha - \dot{\hat{\gamma}}^\alpha}{\gamma^\alpha} = \sum_\beta \phi^2_{\alpha\beta} \dot{s}^\beta; \phi_{\alpha\beta} = \widetilde{\mathbf{m}}^\alpha \cdot \widetilde{\mathbf{s}}^\beta. \tag{16}$$

It is the true slip rate $\dot{\hat{\gamma}}^\alpha$ that is related to dislocation glide through the Orowan equation:

$$\dot{\hat{\gamma}}^\alpha = \rho^\alpha_{\text{mobile}} v^\alpha_{\text{glide}} b^\alpha, \tag{17}$$

and it is on $\dot{\hat{\gamma}}^\alpha$ that power associated with dislocation glide:

$$W_{glide} = \tau^\alpha \dot{\hat{\gamma}}^\alpha, \tag{18}$$

is expanded on, by the Peierls–Nabarro stress τ^α [27,28]. On the other hand, the effective slip γ^α describes the current kinematic state of the material, taking into account the true slip and the changes in the slip geometry caused by climb.

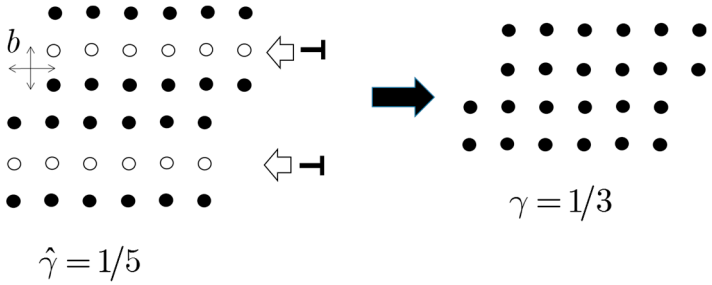

Figure 3. (**Left**) Initial lattice volume $5b \times 5b$ is traversed by an edge dislocation resulting in the true slip $\hat{\gamma} = 1/5$. Two edge dislocations on an orthogonal plane are poised to climb (arrows) and destroy the lattice planes indicated by hollow circles. (**Right**) After the climb, the effective slip is $\gamma = 1/3$.

The plastic velocity gradient in intermediate configuration (15) can now be written as

$$\widetilde{\mathbf{L}}^p = \sum_\alpha \dot{\hat{\gamma}}^\alpha \widetilde{\mathbf{s}}^\alpha \widetilde{\mathbf{m}}^\alpha + \sum_\alpha \dot{s}^\alpha \left[\sum_\beta \gamma^\beta \phi^2_{\beta\alpha} \widetilde{\mathbf{s}}^\beta \widetilde{\mathbf{m}}^\beta - \widetilde{\mathbf{s}}^\alpha \widetilde{\mathbf{s}}^\alpha \right]. \tag{19}$$

2.4. Diffusion and Diffusional Creep Rate

The boundaries of the crystal serve as lattice/vacancy sources and sinks. As discussed in [23], the normal boundary velocity V_n is a scalar field defined on the closure set $\partial\Omega$, and independent of the lattice velocity field. The difference in normal components is the lattice growth rate:

$$g = V_n - \mathbf{n} \cdot \mathbf{v}. \tag{20}$$

The diffusional creep deformation rate tensor is the symmetric rank-2 tensor, constant within each domain Ω, and defined on the basis of the difference between the normal boundary velocity and the normal lattice velocity at the boundary:

$$\mathbf{C} = \frac{1}{\Omega} \int_{\partial\Omega} g \mathbf{nn} d\partial\Omega. \tag{21}$$

In contrast to the locally-defined (fields defined at each point) deformation rates (elastic-compositional and plastic), the diffusional creep deformation rate is defined for each grain. In a polycrystal it is a piecewise constant field with discontinuities across the grain boundaries. On the level of a single grain (mesoscale lattice continuum), the tensor $\mathbf{C}$ describes the lattice growth at the boundary, not the deformation of the lattice. Only on the polycrystal level (macroscale continuum) the name *creep deformation rate* becomes semantically correct. This can be contrasted with the definition of plastic deformation in [21].

The locally-defined (intrinsic) deformation rates are simply the symmetric parts of local lattice velocity gradients. The grain average of the local lattice velocity gradient can be expressed as

$$\langle \mathbf{D} \rangle_\Omega^{intrinsic} = \frac{1}{2\Omega} \int_{\partial\Omega} (\mathbf{vn} + \mathbf{nv}) d\partial\Omega \tag{22}$$

The total deformation rate for the grain is then

$$\langle \mathbf{D} \rangle_\Omega^{total} = \langle \mathbf{D} \rangle_\Omega^{intrinsic} + \mathbf{C}. \tag{23}$$

In the lattice continuum, the local mass balance results in the vacancy diffusion equation [23]. The derivation for the case with lattice sink is given in Appendix B. The diffusion equation reads:

$$\frac{Dc}{Dt} = -F^* \nabla \cdot \mathbf{J} - (1-c)\dot{s}, \tag{24}$$

where $\mathbf{J}$ is the vacancy flux.

The transport theorem with lattice sink is also derived in Appendix B. Let the quantity $Y(\mathbf{x}, t)$ be given per lattice site. Consider the lattice volume $V(t)$, i.e., the volume that follows the prescribed set of lattice sites. The transport theorem has the following form:

$$\frac{D}{Dt} \int\limits_{V(t)} N_L Y dV = \int\limits_{V(t)} N_L \left[\frac{DY}{Dt} - \dot{s} Y \right] dV. \tag{25}$$

For a variable crystal domain $\Omega(t)$, with lattice growing/vanishing at the boundary $\partial\Omega(t)$ with the rate g (20), the transport theorem will have the form:

$$\frac{D}{Dt} \int\limits_{\Omega(t)} N_L Y d\Omega = \int\limits_{\Omega(t)} N_L \left[\frac{DY}{Dt} - \dot{s} Y \right] d\Omega + \int\limits_{\partial\Omega(t)} N_L Y g d\partial\Omega. \tag{26}$$

Applying (26) to the mass density (Appendix B), the mass of a crystal grain will change as

$$\frac{D}{Dt} \int\limits_{\Omega(t)} \rho d\Omega = m \widetilde{N}_L \int\limits_{\partial\Omega(t)} \left[\frac{1-c}{F^*} g + J_n \right] d\partial\Omega, \tag{27}$$

where m is the atomic mass and $J_n = \mathbf{n} \cdot \mathbf{J}$ is the normal vacancy flux at the boundary. Thus, if a single grain is to satisfy mass conservation, then:

$$\int\limits_{\partial\Omega} \left[\frac{1-c}{F^*} g + J_n \right] d\partial\Omega = 0. \tag{28}$$

The weak constraint (28) requires a model for boundary diffusion [23], which is beyond the scope of this paper. The local condition:

$$\frac{1-c}{F^*} g + J_n = 0, \tag{29}$$

implies absence of boundary diffusion by requiring that lattice growth/disappearance at the boundary be directly related to the normal atomic flux (negative of the vacancy flux). The creep deformation rate can then be written as

$$\mathbf{C} = -\frac{1}{\Omega} \int\limits_{\partial\Omega} \frac{F^* J_n}{1-c} \mathbf{n}\mathbf{n} d\partial\Omega. \tag{30}$$

3. Power Balance

3.1. Free Energy

At a constant temperature, the free energy, given per unit volume in intermediate configuration $\widetilde{\Omega}$, depends on concentration and elastic strains: $\Phi(\mathbf{F}^*, c)$. With (13) and (14), the total free energy of a grain with current volume Ω can be written as

$$P = \int\limits_{\widetilde{\Omega}} \Phi(\mathbf{F}^*, c) d\widetilde{\Omega} = \int\limits_{\Omega} \frac{1}{F^*} \Phi(\mathbf{F}^*, c) d\Omega = \int\limits_{\Omega} \frac{1}{\widetilde{N}_L} \Phi(\mathbf{F}^*, c) d\Omega. \tag{31}$$

(Note that interface energy of grain boundaries is not considered here. A discussion of the role of interface energies, including the question of when they can be neglected, can be found in [23].)

The rate of change of the free energy of a grain is derived in the Appendix C:

$$\frac{DP}{Dt} = \int_{\Omega} [\boldsymbol{\sigma} : (\mathbf{v}\nabla) - \Phi'\nabla\cdot\mathbf{J}]d\Omega + \int_{\partial\Omega} \frac{\Phi}{F^*} g d\partial\Omega - \int_{\widetilde{\Omega}} \left[\sum_{\alpha} \hat{\tau}^{\alpha}\dot{\hat{\gamma}}^{\alpha} + \sum_{\alpha} \hat{\Lambda}^{\alpha}\dot{s}^{\alpha}\right] d\widetilde{\Omega}. \tag{32}$$

In (32), $\boldsymbol{\sigma}$ is the symmetric lattice Cauchy stress:

$$\boldsymbol{\sigma} = \frac{1}{F^*}\mathbf{F}^* \cdot \left(\frac{\partial\Phi}{\partial\mathbf{F}^*}\right)^T = \frac{1}{F^*}\left(\frac{\partial\Phi}{\partial\mathbf{F}^*}\right) \cdot \mathbf{F}^{*T}, \tag{33}$$

and the following shorthand notation is introduced:

$$\begin{gathered} \hat{\Lambda}^{\alpha} = \sum_{\beta} \gamma^{\beta}\hat{\tau}^{\beta}\phi^2_{\beta\alpha} + \hat{\sigma}^{\alpha} + \Phi'(1-c) + \Phi; \Phi' = \partial\Phi/\partial c; \\ \hat{\tau}^{\alpha} = \widetilde{\mathbf{m}}^{\alpha} \cdot \widetilde{\mathbf{S}} \cdot \widetilde{\mathbf{s}}^{\alpha}; \hat{\sigma}^{\alpha} = -\widetilde{\mathbf{s}}^{\alpha} \cdot \widetilde{\mathbf{S}} \cdot \widetilde{\mathbf{s}}^{\alpha}; \widetilde{\mathbf{S}} = F^*(\mathbf{F}^{*-1} \cdot \boldsymbol{\sigma} \cdot \mathbf{F}^*)\,. \end{gathered} \tag{34}$$

The non-symmetric stress tensor $\widetilde{\mathbf{S}}$ [17] resolved to appropriate planes and directions gives the resolved shear stress $\hat{\tau}^{\alpha}$ and the normal stress $\hat{\sigma}^{\alpha}$.

3.2. Dissipation and the 2nd Law

Local diffusional dissipation rate in the lattice is modeled simply as proportional to the divergence of flux, while the dissipation rates associated with glide and climb of dislocations are proportional to $\dot{\hat{\gamma}}^{\alpha}$ and $\dot{s}^{\alpha}$:

$$\begin{gathered} D_{diff} = \int_{\Omega} M\nabla\cdot\mathbf{J}d\Omega = \int_{\partial\Omega} MJ_n d\partial\Omega - \int_{\Omega} \nabla M\cdot\mathbf{J}d\Omega\,; \\ D_{climb} = \int_{\widetilde{\Omega}} \sum_{\alpha} \Lambda^{\alpha}\dot{s}^{\alpha} d\widetilde{\Omega}\,; \\ D_{glide} = \int_{\widetilde{\Omega}} \sum_{\alpha} \tau^{\alpha}\dot{\hat{\gamma}}^{\alpha} d\widetilde{\Omega}\,. \end{gathered} \tag{35}$$

In addition to the bulk dissipation, the vacancy creation and absorption at the boundaries must be a dissipative process. Following (29), the dissipation rate at a boundary point can be equivalently assumed to be proportional either to the lattice growth rate g, or to the normal vacancy flux J_n:

$$D_{bdr} = \int_{\partial\Omega} \chi J_n d\partial\Omega\,. \tag{36}$$

The total dissipation rate is then

$$D = \int_{\partial\Omega} (\mathcal{M}+\chi)J_n d\partial\Omega - \int_{\Omega} \nabla\mathcal{M}\cdot\mathbf{J}d\Omega + \int_{\widetilde{\Omega}} \sum_{\alpha} \Lambda^{\alpha}\dot{s}^{\alpha} d\widetilde{\Omega} + \int_{\widetilde{\Omega}} \sum_{\alpha} \tau^{\alpha}\dot{\hat{\gamma}}^{\alpha} d\widetilde{\Omega}. \tag{37}$$

For isothermal processes, the 2nd law of thermodynamics requires

$$D \geq 0. \tag{38}$$

The linear constitutive law with positive mobilities B, β and H:

$$\begin{gathered} \mathbf{J} = -B\nabla\mathcal{M}\,, \dot{s}^{\alpha} = \beta\Lambda^{\alpha}, \beta, B > 0, \text{ in } \Omega\,; \\ J_n = H(\chi+\mathcal{M})\,, \quad H > 0, \text{ on } \partial\Omega\,, \end{gathered} \tag{39}$$

and the slip constitutive law which guaranties $\tau^\alpha \dot{\hat{\gamma}}^\alpha \geq 0$, will satisfy the requirement (38). An acceptable slip constitutive law may be the viscous regularization of a yield condition:

$$\dot{\hat{\gamma}}^\alpha = \gamma_0 \left| \frac{\tau^\alpha}{\tau_Y^\alpha} \right|^m \text{sign}(\tau^\alpha); \gamma_0, \tau_Y^\alpha > 0;\ m \gg 1, \tag{40}$$

accompanied by the appropriate hardening law for $d\tau_Y^\alpha / d\hat{\gamma}^\alpha$ (see, e.g., [16]).

3.3. Power Balance

The boundary tractions **t** expand power on the boundary velocity **V**. The power balance for an isothermal process can be written as

$$\int_{\partial\Omega} \mathbf{t} \cdot \mathbf{V} d\partial\Omega = \frac{DP}{Dt} + D. \tag{41}$$

We define the tangential component of boundary velocity to be equal to the tangential components of lattice velocity, so that, with (29) the power expanded by tractions can be written as

$$\mathbf{t} \cdot \mathbf{V} = t_n g + \mathbf{t} \cdot \mathbf{v} = -t_n \frac{F^*}{1-c} J_n + \mathbf{t} \cdot \mathbf{v}; t_n = \mathbf{t} \cdot \mathbf{n}. \tag{42}$$

Upon substitution of (32), (35), (36) and (42) into (41), the power balance takes the form

$$\begin{aligned} \int_{\partial\Omega} \mathbf{t} \cdot \mathbf{v} d\partial\Omega = \int_\Omega [\boldsymbol{\sigma} : (\mathbf{v}\nabla) + (\mathcal{M} - \Phi')\nabla \cdot \mathbf{J}] d\Omega + \int_{\partial\Omega} \left[\chi + \tfrac{F^* t_n - \Phi}{1-c}\right] J_n d\partial\Omega \\ + \int_{\widetilde{\Omega}} \sum_\alpha (\Lambda^\alpha - \hat{\Lambda}^\alpha) \dot{s}^\alpha d\widetilde{\Omega} + \int_{\widetilde{\Omega}} \sum_\alpha (\tau^\alpha - \hat{\tau}^\alpha) \dot{\hat{\gamma}}^\alpha d\widetilde{\Omega}\,. \end{aligned} \tag{43}$$

4. Principle of Virtual Power and Governing Equations

Following (43), at any instant t, the fields $\mathbf{v}(\mathbf{x}, t)$, $\mathbf{J}(\mathbf{x}, t)$, $\dot{s}^\alpha(\mathbf{x}, t)$ and $\dot{\hat{\gamma}}^\alpha(\mathbf{x}, t)$ are subject to independent variations $\delta\mathbf{v}(\mathbf{x}, t)$, $\delta\mathbf{J}(\mathbf{x}, t)$, $\delta\dot{s}^\alpha(\mathbf{x}, t)$ and $\delta\dot{\hat{\gamma}}^\alpha(\mathbf{x}, t)$, arbitrary except at points where the essential boundary conditions are prescribed (allowable variations). The principle of virtual power provides the weak form of the initial-boundary value problem. The integral equation representing power expanded by actual power conjugates on virtual rates:

$$\begin{aligned} \int_{\partial\Omega} \mathbf{t} \cdot \delta\mathbf{v} d\partial\Omega = \int_\Omega [\boldsymbol{\sigma} : \delta(\mathbf{v}\nabla) + (\mathcal{M} - \Phi')\delta\nabla \cdot \mathbf{J}] d\Omega + \int_{\partial\Omega} \left[\chi + \tfrac{F^* t_n - \Phi}{1-c}\right] \delta J_n d\partial\Omega \\ + \int_{\widetilde{\Omega}} \sum_\alpha (\Lambda^\alpha - \hat{\Lambda}^\alpha) \delta\dot{s}^\alpha d\widetilde{\Omega} + \int_{\widetilde{\Omega}} \sum_\alpha (\tau^\alpha - \hat{\tau}^\alpha) \delta\dot{\hat{\gamma}}^\alpha d\widetilde{\Omega}\,, \end{aligned} \tag{44}$$

must be satisfied for arbitrary allowable variations.

Compared to the problem discussed previously [23], only the last two terms are new. Nevertheless, we summarize all the components of the strong form implied by (44). The usual manipulation and the argument based on independence of variations yields:

- Stress (quasi-) equilibrium with standard boundary conditions:

$$\nabla \cdot \boldsymbol{\sigma} = 0 \text{ in } \Omega; \mathbf{n} \cdot \boldsymbol{\sigma} = \mathbf{t}^0 \text{ or } \mathbf{v} = \mathbf{v}^0 \text{ on } \partial\Omega, \tag{45}$$

- The diffusion potential $\mathcal{M} = \Phi'$ and $\chi = -(F^* t_n - \Phi)/(1-c)$, resulting in the coupled, moving-boundary diffusion problem with an unusual boundary condition:

$$\begin{array}{ll} \frac{Dc}{Dt} = BF^* \nabla^2 \Phi' - (1-c)\dot{s} & \text{in } \Omega\,; \\ \frac{1-c}{F^*} g = B\mathbf{n} \cdot \nabla \Phi' = H\left(\frac{F^* t_n - \Phi}{1-c} - \Phi' \right) & \text{on } \partial\Omega\,, \end{array} \tag{46}$$

- The power conjugate of the true slip rate as the resolved shear stress component of the stress tensor $\widetilde{\mathbf{S}}$:

$$\tau^\alpha = \hat{\tau}^\alpha = \widetilde{\mathbf{m}}^\alpha \cdot \widetilde{\mathbf{S}} \cdot \widetilde{\mathbf{s}}^\alpha, \tag{47}$$

- The power conjugate of the climb/sink rate:

$$\Lambda^\alpha = \hat{\Lambda}^\alpha = \sum_\beta \gamma^\beta \hat{\tau}^\beta \phi^2_{\beta\alpha} + \hat{\sigma}^\alpha + \Phi'(1-c) + \Phi. \tag{48}$$

With constitutive equations for elasticity, slip rate (41) and climb rate (40), this completes the initial-boundary value problem. The diffusion portion of the problem (46) differs from the previously discussed case [23] only by the sink term. The resolved shear stress (47) is the standard concept in crystal plasticity. The climb power conjugate (48) requires a more detailed discussion.

The 2nd term in (48), $\hat{\sigma}^\alpha$, is the normal (compressive) stress on the plane with normal $\widetilde{\mathbf{s}}^\alpha$. Since slip and climb are defined consistently in the intermediate configuration, the relevant stress tensor is $\widetilde{\mathbf{S}}$. Compression on a lattice plane favors the loss of lattice planes, while the tension favors creation of new planes.

The 3rd term in (48), $\Phi'(1-c)$, is recognized as the osmotic stress [29,30]. It is instructive to consider its linearized version (small elastic-compositional deformation gradient and small vacancy concentration), in conjunction with the regular solution model [31]. In that case [23]:

$$\Phi'(1-c) \approx \Phi' \approx kT\widetilde{N}_L \ln \frac{c}{c_0} - 3\eta p \approx kT\widetilde{N}_L \ln \frac{c}{c^p_{eq}} - p, \tag{49}$$

where k is the Boltzman constant, T is the temperature, c_0 and c^p_{eq} are the equilibrium vacancy concentrations at the temperature T—the first at zero pressure, the second at the current pressure p. The Vegard's law coefficient η describes the volumetric compositional strain as $-\eta(c - c_0)$.

The last term in (48) simply accounts for the fact that each lattice site carries internal energy. When a lattice site is lost, its internal energy is dissipated. This term is probably negligible in most cases. Compared to the terms $\hat{\sigma}^\alpha$ and Φ', its relative magnitude is of the order of elastic-compositional strains, which is not expected to exceed 10^{-4}.

Finally, to understand the first term in (48), consider the case where the only non-zero climb rate is $\dot{s}^\alpha$ and the only non-zero slip rate is $\dot{\hat{\gamma}}^\beta$. With (17), the power expenditure from the first term in (48) can then be written as

$$\gamma^\beta \hat{\tau}^\beta \phi^2_{\beta\alpha} \dot{s}^\alpha = \hat{\tau}^\beta (\dot{\gamma}^\beta - \dot{\hat{\gamma}}^\beta). \tag{50}$$

Thus, this term provides the additional power expanded by the resolved shear stress $\hat{\tau}^\beta$ on the difference between the effective and true slip rates, this difference being the result of the climb $\dot{s}^\alpha$ (see Figure 3). Imagine a (cubic) element loaded by tractions $\hat{\tau}^\beta$. The expanded power is $\hat{\tau}^\beta \dot{\gamma}^\beta$. But the power expanded on glide, i.e., the power expanded by the Peirels–Nabarro stress to move dislocations along the slip plane, is $\hat{\tau}^\beta \dot{\hat{\gamma}}^\beta$. The difference is made up for by (50).

Compared to the terms $\hat{\sigma}^\alpha$ and Φ', the relative magnitude of this term is of the order of plastic strains and cannot in general be neglected, except in the initial stages of deformation when plastic strains are small. Its relative importance increases with increasing plastic deformation. This may be puzzling until one recalls that (50) represents power density (i.e., power per unit volume), and

that the changes in volume resulting from lattice loss compensate for increasing power density (50). To illustrate this point, consider the example shown in Figure 4, specifically, the work done and the power expanded by the constant shear stress τ.

The total work (per unit area of the constant horizontal base) is $\tau\gamma h$. The power is

$$(\tau\gamma h)^{\cdot} = \tau\dot{\gamma}h + \tau\gamma\dot{h} = \tau\dot{\gamma}h - \tau\gamma h\dot{s} = \tau h(\dot{\gamma} - \gamma\dot{s}) = \tau h\dot{\hat{\gamma}}, \tag{51}$$

where we have used $\dot{h} = -\dot{s}h$.

Assume ideal plasticity without hardening and constant rates of true slip $\dot{\hat{\gamma}} = const.$, and climb $\dot{s} = const$. (Constant climb rate in this example is not realistic. To sustain the climb rate, vacancies would have to be injected into the crystal at a prohibitive energetic cost. This is ignored in the idealized example, intended only to illustrate the thermodynamics aspect of climb–glide interaction.) Upon solving $\dot{\gamma} = \dot{\hat{\gamma}} + \gamma\dot{s}$, we obtain unbounded exponential increase in effective slip and the slip work density:

$$\tau\gamma = \tau\frac{\dot{\hat{\gamma}}}{\dot{s}}(e^{\dot{s}t} - 1). \tag{52}$$

However, with $h = h_0 e^{-\dot{s}t}$, the total work (per unit base area) is bounded:

$$\tau\gamma h = \tau h_0\frac{\dot{\hat{\gamma}}}{\dot{s}}(1 - e^{-\dot{s}t}) \leq \tau h_0\frac{\dot{\hat{\gamma}}}{\dot{s}}. \tag{53}$$

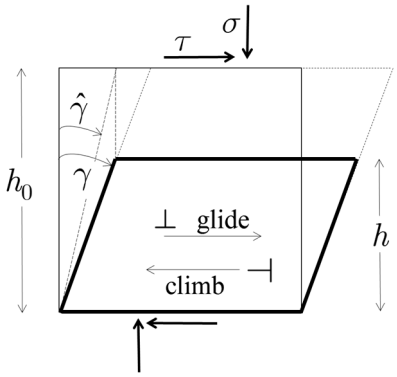

Figure 4. A layer of hypothetical crystal with one active glide system (horizontal slip planes) and one active climb system (vertical slip planes, climb direction to the left), loaded with corresponding constant tractions. Thin solid lines represent the initial shape, thick solid lines represent the current shape. Elastic-compositional deformation is neglected. True and effective slip are shown. To sustain the climb, a continuous stream of vacancies must be injected into the crystal.

5. Conclusions

To describe the coupled dislocation creep and diffusional creep, a lattice continuum theory with a lattice sink/source is developed. The kinematics includes a number of deformation mechanisms: elasticity with diffusion controlled eigenstrains, glide and climb plasticity, and the lattice growth/loss at the boundaries. Building on the previous results for diffusional creep and glide plasticity, we focus on the climb and its interaction with other mechanisms, which can be summarized as follows.

(1) Climb is the sink/source for the lattice itself and is thus embedded in the basic kinematic fields. Given that the vary basis of the continuum is created and vanishes during the deformation process, definition of the Lagrangean variables, specifically the reference and the intermediate configurations, is non-trivial. Moreover, the reference configuration is fictitious and necessarily discontinuous and multiple-valued. The problem is resolved by first defining all fields on the

current configuration, which is real and well-defined. Definition of the deformation gradient as a material field in the current configuration, carried by the lattice and created with the new lattice with continuity, enables the formal definition of other Lagrangean fields.

(2) Climb as the sink/source of vacancies provides the bulk sink/source term in the diffusion equation (which would otherwise only have sinks/sources at grain boundaries).

(3) The coupled climb–glide kinematics requires a distinction between the true slip (glide-only) and the effective slip (the true slip modified by climb). Neither the effective nor the true slips are easily eliminated from the formulation. Thus, when solving the coupled glide–climb problem (presumably numerically), both true and effective slip rates must be updated in each time step.

(4) The glide–climb interaction provides an additional driving force for climb: *the glide coupling force*. Owing to the kinematic coupling, the resolved shear stresses on slip systems not parallel to α expand power on the climb rate $\dot{s}^{\alpha}$.

Finally, note that the present formulation is a simple continuum where slip and climb are not the primary unknown fields, but rather, the state variables evaluated from local constitutive laws. Consequently, the energetics and dissipation associated with dislocation-interface relaxations are not included. These require a size-dependent theory in which slip and climb are independent fields subject to field equations. Such formulations exist for slip [32,33], but not for climb.

Conflicts of Interest: The author declares no conflict of interest.

Appendix A. True Slip and Effective Slip

With reference to Figures 3 and 4, let the current true slip on the only slip system be γ, measured as the number k of Burgers vector lengths b crossed by dislocation passing through the cubic volume $(nb)^3$: $\gamma = kb/(nb)$. Let the small amount of climb Δs on other slip systems destroy some lattice planes parallel to the slip planes, so that the same material now has $(1-\Delta s)nb$ parallel lattice planes. The new value of slip is

$$\gamma + \Delta\gamma = \frac{kb}{(1-\Delta s)nb} = \frac{\gamma}{(1-\Delta s)}.$$

when $\Delta s \ll 1$:

$$\frac{\Delta\gamma}{\gamma} = \frac{1}{1-\Delta s} - 1 \approx \Delta s.$$

Now, interpret $\Delta\gamma/\Delta t$ as the rate of change arising from the specific component of climb on other systems, i.e., the difference between the effective and true slip rates: $\dot{\gamma}^{\alpha} - \dot{\hat{\gamma}}^{\alpha}$. Then, observe that the component Δs which affects the slip system α, is the projection of all climbs to $\widetilde{\mathbf{m}}^{\alpha}$:

$$\frac{\Delta s}{\Delta t} = \widetilde{\mathbf{m}}^{\alpha} \cdot \left[\sum_{\beta} \dot{s}^{\beta} \widetilde{\mathbf{s}}^{\beta} \widetilde{\mathbf{s}}^{\beta} \right] \cdot \widetilde{\mathbf{m}}^{\alpha}.$$

Thus, we obtain (16):

$$\frac{\dot{\gamma}^{\alpha} - \dot{\hat{\gamma}}^{\alpha}}{\gamma^{\alpha}} = \sum_{\beta} \phi_{\alpha\beta}^{2} \dot{s}^{\beta}; \; \phi_{\alpha\beta} = \widetilde{\mathbf{m}}^{\alpha} \cdot \widetilde{\mathbf{s}}^{\beta}.$$

Appendix B. Diffusion, Transport and Mass Balance

The number of atoms per unit volume in the current configuration is $(1-c)N_L$. In the mix of vacancies and atoms with mass m, mass density is given as $\rho = m(1-c)N_L$, so that

$$\frac{D\rho}{Dt} = -mN_L \frac{Dc}{Dt} + m(1-c)\frac{DN_L}{Dt} = -mN_L \frac{Dc}{Dt} - \rho\nabla\cdot\mathbf{v} - \rho\dot{s}. \tag{A1}$$

Let the average velocity of atoms be $\mathbf{v}^a$. The local mass conservation requires:

$$\frac{\partial \rho}{\partial t} = -\nabla \cdot (\rho \mathbf{v}^a) = -\rho \nabla \cdot \mathbf{v}^a - \mathbf{v}^a \cdot \nabla \rho + \mathbf{v} \cdot \nabla \rho - \mathbf{v} \cdot \nabla \rho.$$

The material derivative is then

$$\frac{D\rho}{Dt} = -\rho \nabla \cdot \mathbf{v}^a - (\mathbf{v}^a - \mathbf{v}) \cdot \nabla \rho. \tag{A2}$$

Upon equating (A1) and (A2), we obtain

$$\begin{array}{c} mN_L \frac{Dc}{Dt} = \rho \nabla \cdot (\mathbf{v}^a - \mathbf{v}) + (\mathbf{v}^a - \mathbf{v}) \cdot \nabla \rho - \rho \dot{s} \\ \Rightarrow \frac{Dc}{Dt} = F^* \nabla \cdot \left[\frac{1-c}{F^*} (\mathbf{v}^a - \mathbf{v}) \right] - (1-c)\dot{s} \, . \end{array} \tag{A3}$$

The vacancy flux $\mathbf{J}$, relative to the lattice, is the negative of the atomic flux $\mathbf{J}^a$:

$$\mathbf{J} = -\mathbf{J}^a = -\frac{1-c}{F^*}(\mathbf{v}^a - \mathbf{v}) = \frac{1-c}{F^*}(\mathbf{v}^v - \mathbf{v}). \tag{A4}$$

Substitution of (A4) into (A3) yields the diffusion Equation (24).

Let the quantity $Y(\mathbf{x}, t)$ be a specific quantity given per lattice site. Consider the lattice volume $V(t)$, i.e., the volume that follows the prescribed set of lattice sites. The rate of change of the total quantity is:

$$\frac{D}{Dt} \int\limits_{V(t)} N_L Y dV = \int\limits_{V(t)} \frac{\partial N_L}{\partial t} Y dV + \int\limits_{V(t)} N_L \frac{\partial Y}{\partial t} dV + \int\limits_{\partial V(t)} \mathbf{n} \cdot \mathbf{v} N_L Y d\partial V.$$

Using (5) and (6), we obtain the transport theorem for the material volume with a sink:

$$\begin{array}{l} \frac{D}{Dt} \int\limits_{V(t)} N_L Y dV = - \int\limits_{V(t)} \dot{s} N_L Y dV + \int\limits_{V(t)} N_L \frac{\partial Y}{\partial t} dV + \int\limits_{V(t)} N_L \mathbf{v} \cdot \nabla Y dV \\ = \int\limits_{V(t)} N_L \left[\frac{DY}{Dt} - \dot{s} Y \right] dV \, . \end{array} \tag{A5}$$

For a variable crystal domain $\Omega(t)$, with the lattice growing/vanishing with the rate g at the boundary $\partial\Omega(t)$, the transport theorem will have the form:

$$\frac{D}{Dt} \int\limits_{\Omega(t)} N_L Y d\Omega = \int\limits_{\Omega(t)} N_L \left[\frac{DY}{Dt} - \dot{s} Y \right] d\Omega + \int\limits_{\partial\Omega(t)} N_L Y g d\partial\Omega. \tag{A6}$$

We apply (A6) to the mass density to obtain the mass balance for a grain (27):

$$\begin{array}{l} \frac{D}{Dt} \int\limits_{\Omega} \rho d\Omega = \frac{D}{Dt} \int\limits_{\Omega} m N_L (1-c) d\Omega = \\ = m \int\limits_{\Omega} N_L \left[-\frac{Dc}{Dt} - \dot{s}(1-c) \right] d\Omega + m \int\limits_{\partial\Omega} N_L (1-c) g d\partial\Omega \\ = m \widetilde{N}_L \int\limits_{\Omega} \nabla \cdot \mathbf{J} d\Omega + m \widetilde{N}_L \int\limits_{\partial\Omega} \frac{1-c}{F^*} g d\partial\Omega = m \widetilde{N}_L \int\limits_{\partial\Omega} \left[\frac{1-c}{F^*} g + J_n \right] d\partial\Omega \, . \end{array}$$

Appendix C. Rate of Change of the Free Energy

We seek the time derivative of the total free energy in the variable crystal domain $\Omega(t)$, with the lattice growing/vanishing with the rate g at the boundary $\partial\Omega(t)$. Starting from (31) and applying the transport theorem (A6), and transformations (13) and (14):

$$\begin{aligned}\tfrac{DP}{Dt} &= \tfrac{D}{Dt}\int\limits_{\Omega}\tfrac{N_L}{\widetilde{N}_L}\Phi(\mathbf{F}^*,c)d\Omega\\ &= \int\limits_{\Omega} N_L\left[-\tfrac{\Phi}{\widetilde{N}_L^2}\tfrac{D\widetilde{N}_L}{Dt}+\tfrac{1}{\widetilde{N}_L}\left(\left(\tfrac{\partial\Phi}{\partial\mathbf{F}^*}\right)^T:\tfrac{D\mathbf{F}^*}{Dt}+\tfrac{\partial\Phi}{\partial c}\tfrac{Dc}{Dt}-\dot{s}\Phi\right)\right]d\Omega+\int\limits_{\partial\Omega}\tfrac{\Phi}{F^*}gd\partial\Omega\,.\end{aligned} \tag{A7}$$

Since the change of lattice density can only result from lattice stretching:

$$\frac{DN_L}{Dt} = -N_L\mathrm{tr}\mathbf{L}^*, \tag{A8}$$

the material rate of change of the lattice density in intermediate configuration vanishes: $D\widetilde{N}_L/Dt = 0$. The second term in the integrand of (A7) can be written as

$$\begin{aligned}&\int\limits_{\Omega}\tfrac{1}{F^*}\left(\left(\tfrac{\partial\Phi}{\partial\mathbf{F}^*}\right)^T:\tfrac{D\mathbf{F}^*}{Dt}\right)d\Omega=\int\limits_{\Omega}[\boldsymbol{\sigma}:\mathbf{L}-\boldsymbol{\sigma}:\mathbf{L}^p]d\Omega\\ &=\int\limits_{\Omega}\boldsymbol{\sigma}:(\mathbf{v}\nabla)d\Omega-\int\limits_{\widetilde{\Omega}}F^*(\mathbf{F}^{*-1}\cdot\boldsymbol{\sigma}\cdot\mathbf{F}^*):\widetilde{\mathbf{L}}^p d\widetilde{\Omega}=\int\limits_{\Omega}\boldsymbol{\sigma}:(\mathbf{v}\nabla)d\Omega-\int\limits_{\widetilde{\Omega}}\widetilde{\mathbf{S}}:\widetilde{\mathbf{L}}^p d\widetilde{\Omega}\,,\end{aligned} \tag{A9}$$

with the symmetric lattice Cauchy stress

$$\boldsymbol{\sigma} = \frac{1}{F^*}\mathbf{F}^*\cdot\left(\frac{\partial\Phi}{\partial\mathbf{F}^*}\right)^T = \frac{1}{F^*}\left(\frac{\partial\Phi}{\partial\mathbf{F}^*}\right)\cdot\mathbf{F}^{*T},$$

and the non-symmetric stress tensor $\widetilde{\mathbf{S}} = F^*(\mathbf{F}^{*-1}\cdot\boldsymbol{\sigma}\cdot\mathbf{F}^*)$. We substitute (A9) and the diffusion Equation (24) into (A7). With the shorthand $\Phi' = \partial\Phi/\partial c$:

$$\frac{DP}{Dt} = \int\limits_{\Omega}[\boldsymbol{\sigma}:(\mathbf{v}\nabla)-\Phi'\nabla\cdot\mathbf{J}]d\Omega-\int\limits_{\widetilde{\Omega}}\left[\widetilde{\mathbf{S}}:\widetilde{\mathbf{L}}^p+\Phi'(1-c)+\Phi\dot{s}\right]d\widetilde{\Omega}+\int\limits_{\partial\Omega}\frac{\Phi}{F^*}gd\partial\Omega. \tag{A10}$$

Finally, we substitute (19) for $\widetilde{\mathbf{L}}^p$ into (A10):

$$\begin{aligned}&\tfrac{DP}{Dt}=\int\limits_{\Omega}[\boldsymbol{\sigma}:(\mathbf{v}\nabla)-\Phi'\nabla\cdot\mathbf{J}]d\Omega+\int\limits_{\partial\Omega}\tfrac{\Phi}{F^*}gd\partial\Omega\\ &-\int\limits_{\widetilde{\Omega}}\left[\sum_{\alpha}\dot{\widetilde{\gamma}}^{\alpha}\widetilde{\mathbf{S}}:(\widetilde{\mathbf{s}}^{\alpha}\widetilde{\mathbf{m}}^{\alpha})+\sum_{\alpha}\left(\sum_{\beta}\gamma^{\beta}\phi^2_{\beta\alpha}\widetilde{\mathbf{S}}:(\widetilde{\mathbf{s}}^{\beta}\widetilde{\mathbf{m}}^{\beta})-\widetilde{\mathbf{S}}:(\widetilde{\mathbf{s}}^{\alpha}\widetilde{\mathbf{s}}^{\alpha})+\Phi'(1-c)+\Phi\right)\dot{s}^{\alpha}\right]d\widetilde{\Omega}\,,\end{aligned}$$

and, with the notation (34), we obtain (32).

References

1. Frost, H.J.; Asby, M.F. *Deformation-Mechanism Maps: The Plasticity and Creep of Metals and Ceramics*; Pergamon Press: Oxford, UK, 1982; p. 44.
2. Stouffer, D.C.; Dame, L.T. *Inelastic Deformation of Metals*; John Wiley & Sons: Hoboken, NJ, USA, 1996.
3. Nabarro, F.R.N. Deformation of crystals by the motion of single ions. In *Report of a Conference on Strength of Solids*; The Physical Society: London, UK, 1948; pp. 75–90.
4. Herring, C. Diffusional viscosity of a polycrystalline solid. *J. Appl. Phys.* **1950**, *21*, 437–445. [CrossRef]
5. Coble, R.L. A model for boundary diffusion controlled creep in polycrystalline materials. *J. Appl. Phys.* **1963**, *34*, 1679–1682. [CrossRef]

6. Weertman, J.R. Theory of steady-state creep based on dislocation climb. *J. Appl. Phys.* **1955**, *26*, 1213–1217. [CrossRef]
7. Nabarro, F.R.N. Steady-state diffusional creep. *Philos. Mag.* **1967**, *16*, 231–237. [CrossRef]
8. Edelin, G.; Poirier, J.P. Etude de la montée des dislocations au moyen d'expériences de fluage par diffusion dans le magnésium. *Philos. Mag.* **1973**, *28*, 1203–1210. [CrossRef]
9. Epishin, A.; Link, T. Mechanisms of high-temperature creep of nickel-based superalloys under low applied stresses. *Philos. Mag.* **2004**, *84*, 1979–2000. [CrossRef]
10. Mompiou, F.; Caillard, D. Dislocation-climb plasticity: Modelling and comparison with the mechanical properties of icosahedral AlPdMn. *Acta Mater.* **2008**, *56*, 2262–2271. [CrossRef]
11. Boioli, F.; Carrez, P.; Cordier, P.; Devincre, D.; Gouriet, K.; Hirel, P.; Kraych, A.; Ritterbex, S. Pure climb creep mechanism drives flow in Earth's lower mantle. *Sci. Adv.* **2017**, *3*, e1601958. [CrossRef] [PubMed]
12. Was, G.S. *Fundamentals of Radiation Materials Science: Metals and Alloys*; Springer: Berlin, Germany, 2007.
13. Lowengrub, J.; Truskinovsky, L. Quasi-incompressible Cahn-Hilliard fluids and topological transition. *Proc. R. Soc. Lond. A* **1998**, *454*, 2617–2654. [CrossRef]
14. Lee, E.H. Elastic–plastic deformation at finite strains. *J. Appl. Mech.* **1969**, *36*, 1–6. [CrossRef]
15. Hill, R.; Havner, K.S. Perspectives in the mechanics of elastoplastic crystals. *J. Mech. Phys. Solids* **1982**, *30*, 5–22. [CrossRef]
16. Asaro, R.J. Micromechanics of crystals and polycrystals. *Adv. Appl. Mech.* **1983**, *23*, 1–115.
17. Bassani, J.L. Plastic flow of crystals. *Adv. Appl. Mech.* **1994**, *30*, 191–257.
18. Larché, F.C.; Cahn, J.W. A linear theory of thermochemical equilibrium of solids under stress. *Acta Metall.* **1973**, *21*, 1051–1063. [CrossRef]
19. Larché, F.C.; Cahn, J.W. Thermochemical equilibrium of multiphase solids under stress. *Acta Metall.* **1978**, *26*, 1579–1589. [CrossRef]
20. Larché, F.C.; Cahn, J.W. Interaction of composition and stress in crystalline solids. *Acta Metall.* **1985**, *33*, 331–357. [CrossRef]
21. Berdichevsky, V.; Hazzledine, P.; Shoykhet, B. Micromechanics of diffusional creep. *Int. J. Eng. Sci.* **1997**, *35*, 1003–1032. [CrossRef]
22. Garikipati, K.; Bassman, L.; Deal, M. A lattice-based micromechanical continuum formulation for stress-driven mass transport in polycrystalline solids. *J. Mech. Phys. Solids* **2001**, *49*, 1209–1237. [CrossRef]
23. Mesarovic, S.Dj. Lattice continuum and diffusional creep. *Proc. R. Soc. A* **2016**, *472*, 20160039. [CrossRef] [PubMed]
24. Alankar, A.; Field, D.P.; Zbib, H.M. Explicit incorporation of cross-slip in a dislocation density based crystal plasticity model. *Philos. Mag.* **2012**, *92*, 3084–3100. [CrossRef]
25. Arsenlis, A.; Wirth, B.D.; Rhee, M. Dislocation density-based constitutive model for the mechanical bahaviour of irradiated Cu. *Philos. Mag.* **2004**, *84*, 3517–3635. [CrossRef]
26. Li, D.; Zbib, H.; Sun, X.; Khaleel, M. Predicting plastic flow and irradiation hardening of iron single crystal with mechanism-based continuum dislocation dynamics. *Int. J. Plasticity* **2014**, *52*, 3–17. [CrossRef]
27. Peierls, R.E. The size of a dislocation. *Proc. Phys. Soc.* **1940**, *52*, 34–38. [CrossRef]
28. Nabarro, F.R.N. Dislocations in a simple cubic lattice. *Proc. Phys. Soc.* **1967**, *59*, 256–272. [CrossRef]
29. Lothe, J.; Hirth, J.P. Dislocation climb forces. *J. Appl. Phys.* **1967**, *38*, 845–849. [CrossRef]
30. Gao, Y.; Cocks, A.C.F. Thermodynamic variational approach for climb of an edge dislocation. *Acta Mech. Solida Sin.* **2009**, *22*, 426–435. [CrossRef]
31. Haasen, P. *Physical Metallurgy*, 2nd ed.; Cambridge University Press: Cambridge, UK, 1986.
32. Mesarovic, S.Dj.; Baskaran, R.; Panchenko, A. Thermodynamic coarse-graining of dislocation mechanics and the size-dependent continuum crystal plasticity. *J. Mech. Phys. Solids* **2010**, *58*, 311–329. [CrossRef]
33. Mesarovic, S.Dj. Plasticity of crystals and interfaces: From discrete dislocations to size-dependent continuum theory. *Theor. Appl. Mech.* **2010**, *37*, 289–332. [CrossRef]